STUDIA UBB CHEMIA, LX, 3, 2015 (p. 87-98)
(RECOMMENDED CITATION)

Dedicated to prof. dr. I. C. Popescu
on the occasion of his 70th anniversary

ELECTROCHEMICAL STUDIES ON MODIFIED ORGANO-SILANES COMPOSITE COATINGS FOR ALUMINIUM CORROSION INHIBITION

IOANA MAIOR[a], IOANA-ALINA CIOBOTARU[*], SIMONA CĂPRĂRESCU, ANCA COJOCARU, DĂNUŢ-IONEL VĂIREANU

ABSTRACT. The main objective of this study consists in developing a new anticorrosive protection coating for packaging industry based on deposition of organo-silanes composite film on the metallic material surface. Silane solutions (octyltrietoxysilane OTES and vyniltrietoxysilane VTES) modified with SiC and CeO_2 nanoparticles were applied on a 99.99% aluminium substrate and compared with a sample of aluminium commercially available package (can).
For the analysis of film composition and metal surface Fourier Transform Infrared Spectroscopy (FT-IR) and Scanning Electron Microscopy (SEM) were performed. The results highlighted the film's compactness and its adhesive properties, as well as the favourable effect of nanoparticles in tested coatings.
Corrosion tests on aluminium samples with and without protective coatings, as well as on commercially available aluminium cans were carried out in phosphoric acid 3M using open circuit potential, potentiodynamic curves and Electrochemical Impedance Spectroscopy (EIS) techniques.

Keywords: *corrosion, aluminium, phosphoric acid, silanes, nanoparticles, electrochemical impedance spectroscopy, FT-IR, SEM*

INTRODUCTION

In recent years, various studies have focused on food safety issues. Among them, food packaging has gained an increased interest. One of the most important features of food packaging materials is their ability to

[a] *"Politehnica" University of Bucharest, Faculty of Applied Chemistry and Materials Science, 1–7 Gh. Polizu Str., RO-011061 Bucharest, Romania*
[*] *Corresponding author: ioanaalinaciobotaru@yahoo.com*

remain neutral against the attacks from various additives contained in food (e.g. phosphoric acid as an acidity regulator included in fizzy drinks) or from food itself, where the pH is already low (e.g. citric acid, acetic acid). This fact may be translated and measurable as a corrosion resistance characteristic of the packaging material.

Among food packaging materials, aluminium has proven to be suitable for different types of food content [1] due to the formation of a protective film on the surface during exposure to atmospheric conditions or to different aqueous solutions [1–5] and therefore is used in a large variety of packaging materials [1, 6].

The aluminium oxide self-formed film on metal surface can act as a barrier during corrosion process in mild corrosive environments, but not in aggressive acid media [7, 8]. One of the most efficient methods to prevent metallic corrosion consists in applying films on the metallic substrate [7, 9] and, in addition, these coatings confer improved properties as mechanical strength or optical appearance [9].

An important factor that influences the interaction and the adhesion of films on metallic substrates is the pre-treatment of the substrate. Therefore, prior to the film deposition, surface pre-treatments play an important role in the bonding process [10, 11].

Chromate coating is a common anticorrosive treatment of aluminium alloys [12–14], but due to its high toxicity, in recent years studies have focused on alternative treatments [12], such as silanization, which is an environmentally compliant alternative [11, 15].

Silane coatings are obtained based on hydrolysis and condensation reactions that take place during film formation [16], by forming oxane bonds between metal and silane [17]. Silane coatings have good barrier properties, are easily applied [11] and high anti-corrosion efficiency [18]. They could be used as a single silane without topcoats for 6 month to 1 year, or as surface pre-treatments before painting [18].

The most commonly used coating technique is dip-coating [9] which consists in dipping the metal substrates into pre-hydrolyzed silane/ water/alcohol solution then drying and curing at a certain temperature [12].

Corrosion resistance of silane films can be improved by adding chemicals with good corrosion inhibitor properties [18] such as pre-treated layers (rare earth salts) or active layers (cerium salts) [16]. In order to achieve better anticorrosive resistance properties, the addition of nanoparticles to the surface silane films has been studied [16, 19, 20]. The nanoparticles can be synthesised in the films or added to the pre-treatment solutions. Silica nanoparticles used in silane films deposited on aluminium substrates lead to the improvement of the substrate corrosion properties [19].

In order to developing a new anticorrosive protection coating for packaging industry, the deposition of different organo-silanes composite film on the metallic material surface have been reported in this paper. OTES and VTES silane solutions modified with SiC and CeO_2 nanoparticles were applied on pure aluminium substrate and then compared with a sample of aluminium commercially available package (can). Corrosion tests on aluminium samples with and without protective coatings, as well as on aluminium cans were carried out in 3M phosphoric acid aqueous solution. From the analysis of film composition and of metal surface the results highlighted the film's compactness and its adhesive properties, as well as the favourable effect of nanoparticles in tested coatings.

RESULTS AND DISCUSSION

The composition of the silane films modified with nanoparticles was investigated by FTIR. Figure 1 depicts the FT-IR spectra of aluminium sheet without coating (Al blank or e.p.), aluminium samples coated with silane films with and without nanoparticles and also nanoparticles powder samples. All silane samples showed *peaks* at 1114–1100cm^{-1}, 968–902cm^{-1} and at 3303-3371cm^{-1} corresponding to Si–O–Si, Al–O–Si bonds formed between the silane film and aluminium surface, respectively –OH stretching vibration (Table 1). For silane films modified with SiC and CeO_2 nanoparticles -CH_2 corresponding *peaks* were recorded at 2858 and 2859cm^{-1}. -CH_3 stretching vibration *peaks* were recorded for all silane films at 2924cm^{-1} up to 2973cm^{-1}.

Table 1. FT-IR *peaks*

Bonds	**Wavenumber, cm^{-1}**					
	OTES	OTES SiC 3000	OTES CeO_2 3000	VTES	VTES SiC 3000	VTES CeO_2 3000
–OH	3.303	3.318	3.318	3.307	-	3.371
–CH_3	2.924	2.925	2.926	2.967	2.973	2.967
–CH_2	2.858	2.858	2.859	-	-	-
Si–O–Si	1.114	1.106	1.115	1.105	1.144	1.120
Al–O–Si	902	947	948	968	959	958

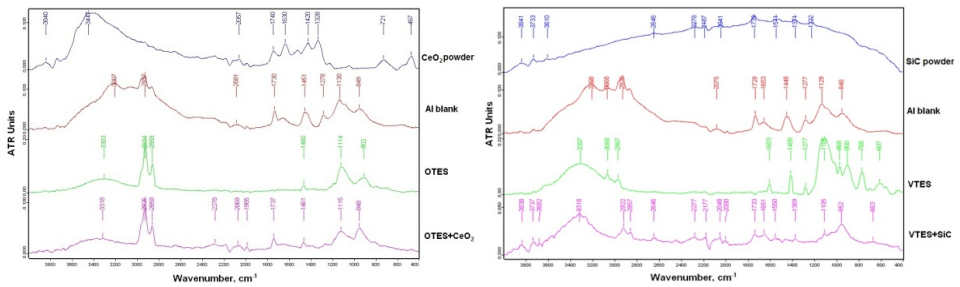

Figure 1. FT-IR spectra for Al e.p., Al OTES 5% and Al OTES 5% modified with CeO_2 (a) and for Al e.p., Al VTES 5% and Al VTES 5% modified with SiC (b)

The surface coating film was investigated by SEM analyses. In Figure 2 are shown SEM micrographs of silane films with and without nanoparticles.

Organic compounds chains exhibit a strong influence on the properties of composite films deposited on aluminium substrate. Synthesized films from octyl and vinyl precursors are forming clusters due to the association of these chains under hydrophobic forces. Films adhesion on aluminium depends on alcoxi-silane nature. A smooth surface is characteristic for silane film without nanoparticles, due to bi-diminesional structure with $–CH_3$ groups on silica surface.

As may be seen in Figure 2, CeO_2 and SiC nanoparticles are incorporated in silane films leading to relatively homogenous silane films.

In addition, synthesized silica nanoparticles exhibit a tridimensional structure with –OH groups. This structure is characterized by a high roughness.

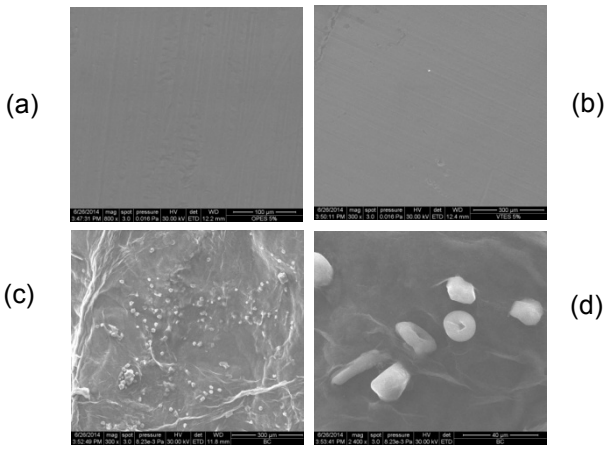

Figure 2. SEM micrographs of silane films deposited on aluminium substrate: (a) OTES 5%, (b) VTES 5%, (c) VTES 5% modified with CeO_2 and (d) VTES 5% modified with SiC

In Figure 3 are shown the variation of potential in time.

As shown in figure 3, initially, the potential decreases, and after 5 minutes increases to more electropositive values. After 20-25 minutes, it can be observed a stabilization of potential at higher values than for uncoated aluminium sample. For the blank aluminium sheet, the potential increases in time until it reaches a constant value, lower than the coated samples.

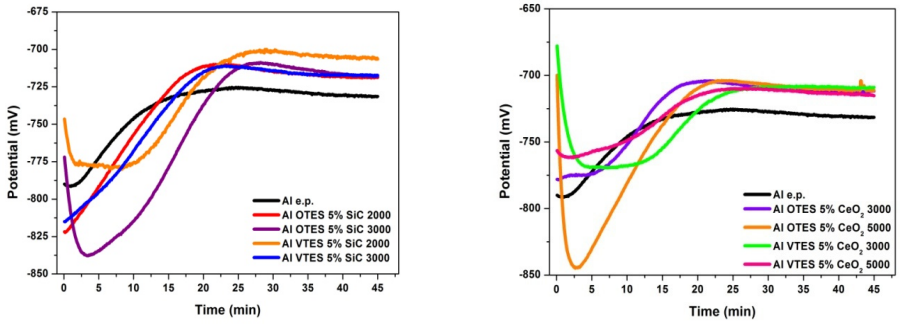

(a) (b)

Figure 3. Variation of potential in time for Al e.p., Al can and Al with silanes modified with SiC (a) and with CeO_2 (b) in H_3PO_4 3M

In Figures 4–6 are presented the Nyquist plots registered in H_3PO_4 3M.

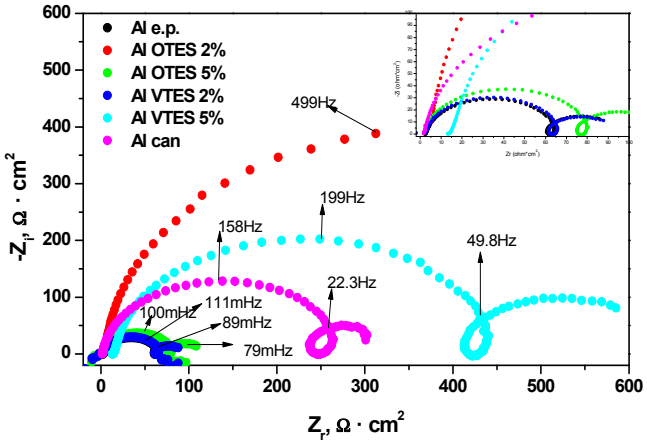

Figure 4. Nyquist plots for Al, Al with silane films and commercially available aluminium cans samples in H_3PO_4 3M

Nyquist plots also show that silane films modified with nanoparticles samples have higher polarization resistance than aluminium samples, indicating a charge transfer process which controls aluminium corrosion.

Rp is the polarization resistance at the electrode/solution interface and represents the diameter of the semicircle calculated from the circular regression applied to the Nyquist plots.

In this particular case, the polarization resistance was calculated using the circular regression applied to the experimental points, taking into consideration the points up to the second intersection of the semicircle with the real impedance axis.

Rp can be used as a quantitative parameter to compare the corrosion resistance of metals under various conditions. This parameter is used to describe the corrosion resistance of the investigated sample, a higher value indicating a better corrosion resistance.

Polarisation resistances of silane films modified with CeO_2, of VTES 2% and OTES 5% have smaller values than the commercially available aluminium cans. Higher polarisation resistance values than the commercially available aluminium cans were obtained for OTES 2%, VTES 5% and VTES 5% modified with SiC. Bode plots (Figure 5) confirm the estimated values of polarisation resistance from Nyquist plots. Also, they confirm the existence of two time constants corresponding to the two processes highlighted by the Nyquist plots.

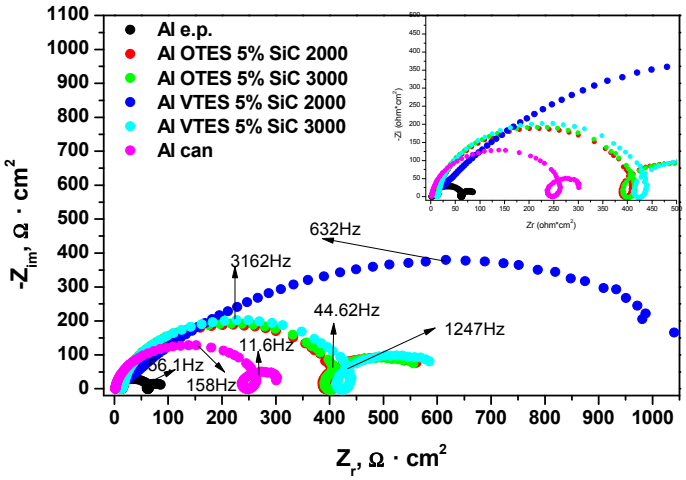

Figure 5.a. Nyquist plots for Al, Al with silane films modified with SiC and commercially available aluminium cans samples in H_3PO_4 3M.

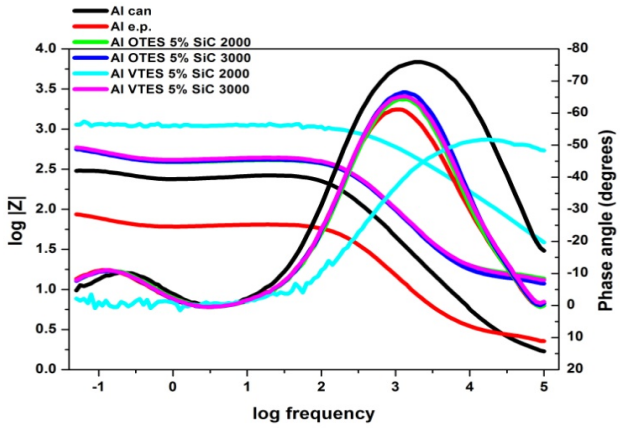

Figure 5.b Bode plots for Al, Al with silane films modified with SiC and commercially available aluminium cans samples in H_3PO_4 3M.

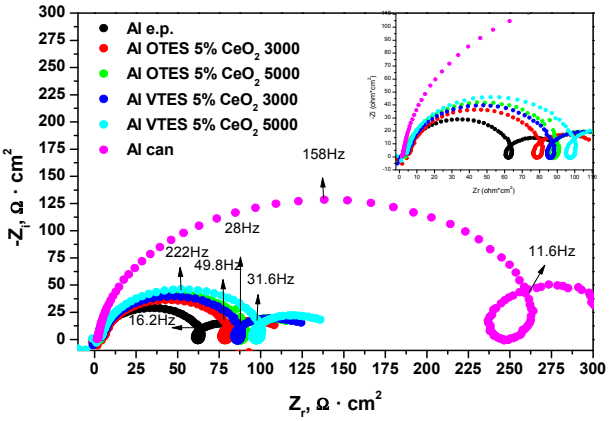

Figure 6. Nyquist plots for Al, Al with silane films modified with CeO_2 and commercially available aluminium cans samples in H_3PO_4 3M

The impedance plots consist of two capacitive loops at high and low frequencies and an inductive loop at medium frequencies. These loops are not perfect semicircles, which can be attributed to dispersion phenomena.

The high frequency capacitive loop is attributed to the charge transfer process during corrosion and to the formation of an oxide layer. The oxide layer can be considered a parallel circuit which consists of a resistance (due to ionic conduction) in oxide layer and a condenser (due to dielectric properties).

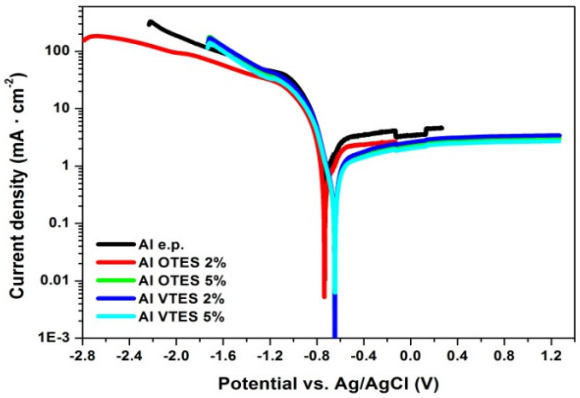

Figure 7. Potentiodynamic polarization curves for Al e.p., Al with silane films and commercially available aluminium cans in H_3PO_4 3M

This loop is attributed to interface reactions, mainly to a three–step aluminium oxidation at metal/oxide/electrolyte interface.

The medium frequencies inductive loop may be attributed to the relaxation of the charge intermediates adsorbed on the electrode surface similar findings are presented in details in [21]. The low frequency capacitive loop may be attributed to a change in the double layer capacitance due to the possible existence of an oxide layer on the metallic surface [22, 23].

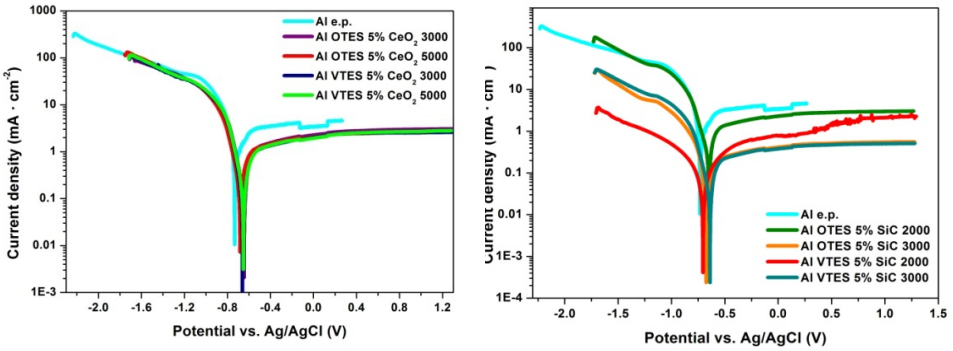

(a) (b)

Figure 8. Potentiodynamic polarization curves for Al e.p., Al with silane films modified with CeO_2 (a) and SiC (b) and commercially available aluminium cans in H_3PO_4 3M

The efficiency of silane coatings on the corrosion reactions was determined by polarization techniques. Potentiodynamic polarization curves are plotted in figures 7 and 8. The potentiodynamic parameters such as corrosion potential (ε_{corr}), cathodic and anodic Tafel slopes (b_c and b_a), corrosion current density (i_{corr}), were obtained from Tafel plots and the inhibition efficiency values IE(%), were calculated using equation 1. The results are presented in Table 2.

Table 2. Electrochemical parameters calculated from Tafel polarization curves on aluminium in 3M phosphoric acid for different silane coatings

Samples	ε_{cor}, mV vs. Ag/AgCl	i_{cor}, μA·cm^{-2}	β_a, mV·dec^{-1}	$-\beta_c$, mV·dec^{-1}	p, mm·y^{-1}	IE,%
Al e.p.	–660	264.90	167.80	127.30	2.88	-
OTES 2%	–739	218.60	64.10	49.40	2.38	17.47
OTES 5%	–651	132.48	51.10	69.30	1.44	49.98
OTES 5% 2000 SiC	–676	16.24	54.70	47.10	0.18	93.86
OTES 5% 3000 SiC	–649	16.51	46.10	55.50	0.18	93.76
OTES 5% 3000 CeO_2	–634	107.12	48.10	65.00	1.16	59.57
OTES 5% 5000 CeO_2	–685	77.59	49.20	54.30	0.84	70.71
VTES 2%	–649	142.39	50.40	69.60	1.55	46.24
VTES 5%	–649	120.98	54.00	66.70	1.32	54.32
VTES 5% 2000 SiC	–717	12.22	48.90	56.20	0.15	95.38
VTES 5% 3000 SiC	–708	13.73	52.00	60.90	0.15	94.81
VTES 5% 3000 CeO_2	–663	62.75	49.80	51.90	0.68	76.31
VTES 5% 5000 CeO_2	–656	68.62	48.90	53.10	0.75	74.09

The inhibition efficiency was calculated using the following equation:

$$IE\ (\%) = \left(1 - \frac{i_{corr}}{i^{0}_{corr}}\right) \cdot 100 \quad (1)$$

where i_{corr} and i^{0}_{corr} are the corrosion current densities obtained in uninhibited and inhibited solutions, respectively. The corrosion rate was calculated using the following equation:

$$p\ (mm/year) = \frac{3270 \cdot M \cdot i_{corr}}{\rho \cdot Z} \quad (2)$$

where 3270 is a constant that defines the unit of corrosion rate, i_{corr} is the corrosion current density in A cm^{-2}, ρ is the density of the corroding material (g cm^{-3}),M is the atomic mass of the metal and Z is the number of electrons transferred per atom.

The smallest value of the corrosion current was recorded for VTES 5% modified with 2000 µg/L SiC. Regardless of the nature of silane, for a concentration of 5% and for the maximum concentration of SiC (3000 µg/L), it can be observed a similar behaviour on both anodic and cathodic curve, leading to small values of the corrosion rate and to achieving the passivation state after a slow evolution in a shorter time (Figure 8).

There was no remarkable shift in the corrosion potential value (ε_{corr}) with respect to the uncoated aluminium sample. The maximum shift is less than ±85 mV. Both anodic and cathodic polarizations are influenced simultaneously and have a similar behaviour, which indicate the influence of coatings on both the anodic and the cathodic reactions.

CONCLUSIONS

FT-IR spectra confirmed the presence of functional groups $–CH_2$, $–CH_3$, –OH and also the presence of Si–O–Si and Al–O–Si bonds.

SEM micrographs confirmed the incorporation of nanoparticles in silane films that led to a certain roughness of films surface.

Electrochemical studies showed a better corrosion behaviour of aluminium with silane modified with SiC than the ones modified with CeO_2 in H_3PO_4 3M. Aluminium with OTES 5% and 2000 SiC has a polarization resistance higher than the commercially available aluminium cans.

Nanoparticles concentration is an important factor in establishing the final properties of the film. The excess of nanoparticles can lead to opposite effects (VTES 5% modified with 5000 CeO_2 has a bigger value of corrosion current than VTES 5% modified with 3000 CeO_2).

EXPERIMENTAL SECTION

The aluminium sheets consisted of aluminium of electrolytic purity (Al 99.9%, with an active surface of 0.5cm^2). Prior to deposition, the substrate was immersed in an alkaline solution (NaOH), then in distilled water, followed by cleaning with ethanol and distilled water using an ultrasonic apparatus. The coatings used in this study are silane solutions of octyltrietoxysilane – OTES and vyniltrietoxysilane – VTES, provided by Sigma Aldrich, modified with SiC and CeO_2 nanoparticles. The concentration of tested silane solutions were of 2 and 5% in ethanol. The maximum concentration of silane solutions were functionalized with SiC and CeO_2 of 2000, 3000 µg/L SiC, respectively 3000, 5000 µg/L CeO_2 concentrations (referred to as SiC 2000, SiC 3000, CeO_2 3000 and CeO_2 5000). The nanoparticles were dispersed in silanes by means of an ultrasonic apparatus. The silane films were deposited on the aluminium substrate by deep-coating procedure for 10 minutes.

The FT-IR spectra were recorded using a Fourier Transforms Infrared spectrometer (Tensor 37 Bruker) in transmission mode (ATR), in the spectral range of 400 – 4000 cm^{-1}. Samples of nanoparticles powder were analysed mixed with KBr.

The surface morphology of silane films was examined on a SIRION Field Emission Scanning Electron Microscope (SEM) produced by FEI Co. Ltd.

Corrosion rate tests were carried out at room temperature (24 ± 2°C) in 3M H_3PO_4 solution as a substitute (stimulant) for water-based food and drinks. The electrochemical measurements were carried out in a three-electrode configuration electrochemical cell consisting of a working electrode (the aluminium sheet with an active area equal to 0.5cm^2), an Ag/AgCl saturated electrode (used as reference electrode, provided by Radiometer Analytical) and a platinum counter electrode (Radiometer Analytical, 1.13cm^2 active area). These studies were performed with a VoltaLab 40 PGZ301 potentiostat, connected to a computer that uses VoltaMaster 4.0 software for data processing.

EIS measures the response of the electrochemical system within a frequency range of 100 kHz – 1Hz using a 10mV a.c. potential excitation. The open circuit potential was measured for over 45 minutes. Potentiodynamic polarization curves were plotted at a scan rate of 10mV/min, starting from cathodic potential.

REFERENCES

1. European Food Safety Authority, *Safety of aluminium from dietary intake,* The EFSA J., **2008**, *754*, 1.
2. M.K. Awad, M.S. Metwally, S.A. Soliman, El-Zomrawy, M.A. Bedair, *J. Ind. and Eng. Chem.*, **2014**, *20*, 796.
3. M. Whelan, J. Cassidy, B. Duffy, *Surface & Coatings Technology*, **2013**, *235*, 86.
4. M. Whelan, K. Barton, J. Cassidy, J. Colreavy, B. Duffy, *Surface & Coatings Technology*, **2013**, *227*, 75.
5. M.A. Amin, Q. Mohsen, O.A. Hazzazi, *Materials Chemistry and Physics*, **2009**, *114*, 908.
6. L. Bouchama, N. Azzouz, N. Boukmouche, J.P. Chopart, A.L. Daltin, Y. Bouznit, *Surface and Coatings Technology*, **2013**, *235*, 676.
7. Y. Wang, Y. Li, F. Wang, *E-Journal of Chemistry*, **2012**, *9*, 435.
8. X. Li, S. Deng, X. Xie, *Corrosion Science*, **2014**, *81*, 162.
9. D. Wang, G.P. Bierwagen, *Progress in Organic Coatings*, **2009**, *64*, 327.
10. W.J. van Ooij, D. Zhu, M. Stacy, A. Seth, T. Mugada, J. Gandhi, P. Puomi, *Tsinghua Science and Technology*, **2005**, *10(6)*, 639.
11. J.B. Bajat, V.B. Miskovic-Stankovic, Z. Kacarevic-Popovic, *Corrosion Science*, **2008**, *50*, 2078.
12. J.M. Hu, L. Liu, J.Q. Zhang, C.N. Cao, *Electrochimica Acta*, **2006**, *51*, 3944.
13. B. Valdez, S. Kiyota, M. Stoytcheva, R. Zlatev, J.M. Bastidas, *Corrosion Science*, **2014**, *87*, 141.
14. L.M. Palomino, P.H. Suegama, I.V. Aoki, M.F. Montemor, H.G. De Melo, *Corrosion Science*, **2009**, *51*, 1238.
15. J.M. Hu, L. Liu, J.Q. Zhang, C.N. Cao, *Progress in Organic Coatings*, **2007**, *58*, 265.
16. L. Liu, J.M. Hu, J.Q. Zhang, C.N. Cao, *Electrochimica Acta*, **2006**, *52*, 538.
17. G. Pan, D.W. Schaefer, *Thin Solid Films*, **2006**, *503*, 259.
18. P.H. Suegama, A.A.C. Recco, A.P. Tschiptschin, I.V. Aoki, *Progress in Organic Coatings*, **2007**, *60*, 90.
19. M.F. Montemor, M.G.S. Ferreira, *Progress in Organic Coatings*, **2008**, *63*, 330.
20. P.H. Suegama, V.H.V. Sarmento, M.F. Montemor, A.V. Benedetti, H.G. de Melo, I.V. Aoki, C.V. Santili, *Electrochimica Acta*, **2010**, *55*, 5100.
21. A. Lasia, Electrochemical Impedance Spectroscopy and Its Applications, in Modern Aspects of Electrochemistry, B.E. Conway, J. Bockris, and R.E. White, Eds., *Kluwer Academic/Plenum Publishers*, New York, **1999**, *32*, 143-248.
22. D. Prabhu, P. Rao, *Journal of Environmental Chemical Engineering*, **2013**, *1*, 676.
23. A.A. Mohammed, Q. Mohsen, O.A. Hazzazi, *Materials Chemistry and Physics*, **2009**, *114*, 908.